Structural Engineering and Mechanics, *Vol. 61, No. 1 (2017) 49-63*
DOI: https://doi.org/10.12989/sem.2017.61.1.049

Mechanical behaviour of FGM sandwich plates using a quasi-3D higher order shear and normal deformation theory

Tahar Hassaine Daouadji*[1,2] and Belkacem Adim[1,2]

[1]*Département de Génie Civil, Université Ibn Khaldoun Tiaret, BP 78 Zaaroura, 14000 Tiaret, Algérie*
[2]*Laboratoire de Géomatique et Développement Durable, Université Ibn Khaldoun de Tiaret, Algérie*

(Received June 5, 2016, Revised July 21, 2016, Accepted September 10, 2016)

Abstract. This paper presents an original hyperbolic (first present model) and parabolic (second present model) shear and normal deformation theory for the bending analysis to account for the effect of thickness stretching in functionally graded sandwich plates. Indeed, the number of unknown functions involved in these presents theories is only five, as opposed to six or even greater numbers in the case of other shear and normal deformation theories. The present theory accounts for both shear deformation and thickness stretching effects by a hyperbolic variation of ail displacements across the thickness and satisfies the stress-free boundary conditions on the upper and lower surfaces of the plate without requiring any shear correction factor. It is evident from the present analyses; the thickness stretching effect is more pronounced for thick plates and it needs to be taken into consideration in more physically realistic simulations. The numerical results are compared with 3D exact solution, quasi-3-dimensional solutions and with other higher-order shear deformation theories, and the superiority of the present theory can be noticed.

Keywords: higher-order theories; shear deformation theory of sandwich plates; functionally graded material

1. Introduction

The concept of Sandwich construction is one of the most functional forms of composite structures developed by the composite industry. It has attained broad acceptance in aerospace and many other industries and it is widely employed in aircraft and space vehicles, ships, boats, cargo containers, and residential constructions. Sandwich composite construction offers great potential for large civil infrastructure projects such as industrial buildings and vehicular bridges. Sandwich structures represent a special form of a layered structure that consists of two thin stiff and strong face sheets separated by a thin and a relatively thick, lightweight, and compliant core material. In modern sandwich structures the faces are usually made of metal or laminated composite materials, and typically a compliant compressible core made of a low-strength honeycomb type material or polymeric foam. The faces and the core are joined by adhesive bonding, which ensures the load transfer between the sandwich constituent parts. However, the demand for improved structural efficiency in many engineering fields has resulted in the development of a new class of materials, called functionally graded materials (FGMs).

Recently, the researches on functionally graded material plates have received substantial attention, and an extensive spectrum of plate theories has been introduced based on the classical plate theory and shear deformation plate theory. The classical plate theory (CPT) neglects shear deformations and can lead to inaccurate results for moderately thick plates. The First-order shear deformation theory (FSDT) Reissner (1945) and Mindlin (1951), considers the transverse shear deformation effects, but needs a shear correction factor in order to satisfy the zero transverse shear stress boundary conditions at the top and bottom of the plate. Many studies of the mechanical behavior of plates have been carried out using FSDT (Della Croce 2004, Tounsi, Menaa *et al.* 2012, Rashidi, Shooshtari *et al.* 2012, Bouazza 2014, Bourada 2015, Hamidi 2015, Mahi 2015). To avoid the use of shear correction factors, several higher-order shear deformation plate theories (HSDTs) have been proposed such as the theory propounded by Nelson and Lorch (1974) with nine unknowns, Lo, Christensen *et al.* (1977) with eleven unknowns, Reddy (1984) with five unknowns. Some higher order theories based on Carrera's unified Formulation (CUF) such as proposed in Refs. (Neves, Ferreira *et al.* 2012, Reddy 2000, Benyoucef, Mechab *et al.* 2010, Ait Amar 2015, Tounsi 2013, Bellifa 2015, Benoun 2016, Bouazza 2015, Bouderba 2015, Abdelhak 2015) have been used also to study FGM structures. The majority of HSDTs used to investigate FGM plate mechanics have the same five unknowns. The resulting equations of motion are much more complicated than those yielded with FSDT. In addition, it should be noted that the above-mentioned two-dimensional plate theories discard the thickness stretching effect as they consider a constant transverse displacement through the thickness. This assumption is appropriate for thin or moderately thick FGM plates, but is inadequate for thick FGM plates (Qian 2004). The importance of the thickness stretching effect in FGM plates has been

*Corresponding author, Professor
E-mail: daouadjitah@yahoo.fr

Copyright © 2017 Techno-Press, Ltd.
http://www.techno-press.org/?journal=sem&subpage=8 ISSN: 1225-4568 (Print), 1598-6217 (Online)

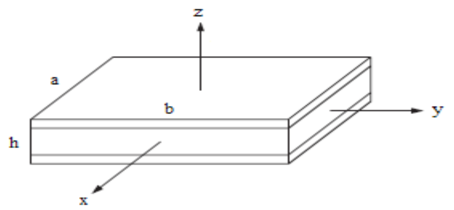

Fig. 1 Geometry of rectangular FGM sandwich plate with uniform thickness in the rectangular Cartesian coordinates

identified succinctly in the work of Carrera, Brischetto *et al.* (2011). This effect plays a significant role in thick FGM plates and should be taken into consideration. In general, higher order shear and normal deformation theories which consider thickness stretching effect can be implemented using the unified formulation initially proposed by Carrera (2011). Many higher order shear and normal deformation theories have been proposed in the literature, these theories are cumbersome and computation-ally expensive since they invariably generate a host of unknowns (e.g., theories by Reddy (2000) with eleven unknowns; and Neves, Ferreira *et al.* (2012) with nine unknowns). Although some well-known quasi-three-dimensional theories developed by Zenkour (2007) and recently by Mantari and Guedes Soares (2014) have six unknowns, they are still more complicated than the FSDT. Thus, there is a scope to develop an accurate higher order shear and normal deformation theory, which is relatively simple to use and simultaneously retains important physical characteristics. Indeed, Thai and Kim (2013) presented recently a quasi-3D sinusoidal shear deformation theory with only five unknowns for bending behavior of FGM plates.

In this present research, a simple quasi -3D trigonometric shear and normal deformation theory with only five unknowns is developed for FGM sandwich plates. Contrary to the four-variable refined theories elaborated in (Tlidji, Hassaine Daouadji *et al.* 2014, Benferhat 2015), where the stretching effect is neglected, in the current investigation this so-called "stretching effect" is taken into consideration. The present theory complies with the tangential stress-free boundary conditions on the plate boundary surface, and thus a shear correction factor is not required. The plate governing equations and their boundary conditions are derived by employing the principle of virtual work. Navier-type analytical solution is obtained for plates subjected to bi-sinusoidal transverse load for simply supported boundary conditions. The results of present optimized higher order shear deformation theory are compared with 3D exact, quasi-exact, and with other closed-form solution published in the literature.

2. Problem formulation for FGM sandwich plates

2.1 Geometrical configuration

Consider the case of a uniform thickness, rectangular FGM sandwich plate composed of three microscopically heterogeneous layers referring to rectangular coordinates (x, y, z) as shown in Fig. 1. The top and bottom faces of the plate are at $z=\pm h/2$, and the edges of the plate are parallel to axes x and y. The sandwich plate is composed of three elastic layers, namely, ''Layer 1'', ''Layer 2'', and ''Layer 3'' from bottom to top of the plate. The vertical ordinates of the bottom, the two interfaces, and the top are denoted by $h_1=-h/2$, h_2, h_3, $h_4=h/2$, respectively. For the brevity, the ratio of the thickness of each layer from bottom to top is denoted by the combination of three numbers, i.e., ''1-0-1'', ''2-1-2'' and so on. As shown in Fig. 2, two types A and B are considered in the present study:

- Type A: FGM facesheet and homogeneous core
- Type B: Homogeneous facesheet and FGM core

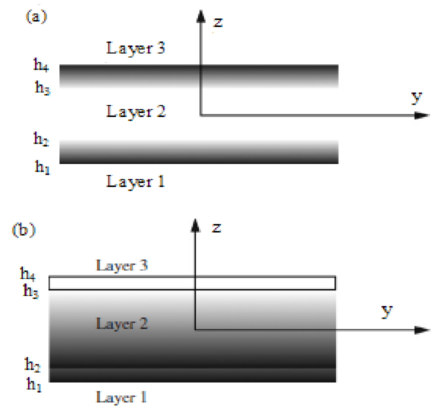

Fig. 2 The material variation along the thickness of the FGM sandwich plate: (a) FGM face sheet and homogeneous core (b) homogeneous face sheet and FGM core

2.2 Material properties

The properties of FGM vary continuously due to gradually changing the volume fraction of the constituent materials, usually in the thickness direction only. Power-law function is commonly used to describe these variations of materials properties. The sandwich structures made of two types of power-law FGMs mentioned before are discussed as follows.

2.2.1 Type A: power-law FGM face sheet and homogeneous core

The volume fraction of the FGMs is assumed to obey a power-law function along the thickness direction

$$V^{(1)}=\left(\frac{z-h_1}{h_2-h_1}\right)^p,\quad z\in[h_1,h_2] \tag{1a}$$

$$V^{(2)}=1,\ z\in[h_2,h_3] \tag{1b}$$

$$V^{(3)}=\left(\frac{z-h_4}{h_3-h_4}\right)^p,\quad z\in[h_3,h_4] \tag{1c}$$

Where $V^{(k)}$, (k=1,2,3) denotes the volume fraction function of layer k; p is the volume fraction index

($0 \le p \le +\infty$), which dictates the material variation profile through the thickness.

2.2.2 Type B: homogeneous facesheet and power-law FGM core

The volume fraction of the FGMs is assumed to obey a power-law function along the thickness direction

$$V^{(1)} = 0 \,, \quad z \in [h_1, h_2] \tag{2a}$$

$$V^{(2)} = \left(\frac{z - h_2}{h_3 - h_2} \right)^p \,, \quad z \in [h_2, h_3] \tag{2b}$$

$$V^{(3)} = 1 \quad z \in [h_3, h_4] \tag{2c}$$

In which $V^{(k)}$, and p are as same as defined in Eq. (1).

The effective material properties, like Young's modulus E, and Poisson's ratio ν, then can be expressed by the rule of mixture (Marur 1999) as

$$P^{(k)}(z) = P_2 + (P_1 - P_2) V^{(k)} \tag{3}$$

Where $P^{(k)}$ is the effective material property of FGM of layer k. For type A, P_1 and P_2 are the properties of the top and bottom faces of layer 1, respectively, and vice versa for layer 3 depending on the volume fraction $V^{(k)}$, (k=1,2,3). For type B, P_1 and P_2 are the properties of layer 3 and layer 1, respectively. These two types of FGM sandwich plates will be discussed later in the following sections. For simplicity, Poisson's ratio of plate is assumed to be constant in this study for that the effect of Poisson's ratio on the deformation is much less than that of Young's modulus (Delale and Erdogan 1983).

2.3 Basic assumptions

The displacement field of the present theory is chosen based on the following assumptions:

- The transverse displacements are partitioned into bending, shear and stretching components;
- The in-plane displacement is partitioned into extension, bending and shear components;
- The bending parts of the in-plane displacements are similar to those given by CPT;
- The shear parts of the in-plane displacements give rise to the trigonometric variations of shear strains and hence to shear stresses through the thickness of the plate in such a way that the shear stresses vanish on the top and bottom surfaces of the plate.

2.4 Kinematics and constitutive equations

Based on these assumptions, the following displacement field relations can be obtained

$$\begin{aligned} u(x,y,z) &= u_0(x,y) - z\frac{\partial w_b}{\partial x} - f(z)\frac{\partial w_s}{\partial x} \\ v(x,y,z) &= v_0(x,y) - z\frac{\partial w_b}{\partial y} - f(z)\frac{\partial w_s}{\partial y} \\ w(x,y,z) &= w_b(x,y) + w_s(x,y) + g(z) w_z(x,y) \end{aligned} \tag{4}$$

Where u_0 and v_0 denote the displacements along the x and y coordinate directions of a point on the mid-plane of the plate; w_b and w_s are the bending and shear components of the transverse displacement, respectively; and the additional displacement w_z accounts for the effect of normal stress. In this study, the shape functions $f(z)$ represents shape functions determining the distribution of the transverse shear strains and stresses along the thickness and is given as :

Present model 1: The function $f(z)$ is an hyperbolic shape function (Hassaine Daouadji 2013) (Hyperbolic Shear Deformation Theory)

$$f(z) = z\left[1 + \frac{3\pi}{2}\sec h^2\left(\frac{1}{2}\right)\right] - \frac{3\pi}{2} h \tanh\left(\frac{z}{h}\right) \tag{5a}$$

Present model 2: The function $f(z)$ is an parabolic shape function (Parabolic Shear Deformation Theory)

$$f(z) = z - z\left(1 - \frac{4z^2}{3h^2}\right) \tag{5b}$$

The non-zero strains associated with the new displacement field in Eq. (4) are

$$\begin{Bmatrix} \varepsilon_x \\ \varepsilon_y \\ \gamma_{xy} \end{Bmatrix} = \begin{Bmatrix} \frac{\partial u_0}{\partial x} \\ \frac{\partial v_0}{\partial y} \\ \frac{\partial u_0}{\partial y} + \frac{\partial v_0}{\partial x} \end{Bmatrix} - z \begin{Bmatrix} \frac{\partial^2 w_b}{\partial x^2} \\ \frac{\partial^2 w_b}{\partial y^2} \\ 2\frac{\partial^2 w_b}{\partial x \partial y} \end{Bmatrix} - f(z) \begin{Bmatrix} \frac{\partial^2 w_s}{\partial x^2} \\ \frac{\partial^2 w_s}{\partial y^2} \\ 2\frac{\partial^2 w_s}{\partial x \partial y} \end{Bmatrix} \tag{6a}$$

$$\begin{Bmatrix} \gamma_{yz} \\ \gamma_{xz} \end{Bmatrix} = \left(1 - \frac{\partial f(z)}{\partial z}\right) \begin{Bmatrix} \frac{\partial w_s}{\partial y} + \frac{\partial w_z}{\partial y} \\ \frac{\partial w_s}{\partial x} + \frac{\partial w_z}{\partial x} \end{Bmatrix} \tag{6b}$$

$$\varepsilon_z = \frac{\partial g(z)}{\partial z} \varepsilon_z^0 = g'(z).w_z \tag{6c}$$

The linear constitutive relations of a FG plate can be written as

$$\begin{Bmatrix} \sigma_x \\ \sigma_y \\ \sigma_z \\ \sigma_{yz} \\ \sigma_{xz} \\ \sigma_{xy} \end{Bmatrix} = \begin{bmatrix} C_{11} & C_{12} & C_{13} & 0 & 0 & 0 \\ C_{12} & C_{22} & C_{23} & 0 & 0 & 0 \\ C_{13} & C_{23} & C_{33} & 0 & 0 & 0 \\ 0 & 0 & 0 & C_{44} & 0 & 0 \\ 0 & 0 & 0 & 0 & C_{55} & 0 \\ 0 & 0 & 0 & 0 & 0 & C_{66} \end{bmatrix} \begin{Bmatrix} \varepsilon_x \\ \varepsilon_y \\ \varepsilon_z \\ \gamma_{yz} \\ \gamma_{xz} \\ \gamma_{xy} \end{Bmatrix} \tag{7}$$

Where (σ_x, σ_y, σ_z, τ_{yz}, τ_{xz}, τ_{xy}) and (ε_x, ε_y, ε_z, γ_{yz}, γ_{xz}, γ_{xy}) are the stress and strain components, respectively. The computation of the elastic constants C_{ij} depends on which assumption of ε_z we consider. If ε_z=0, then C_{ij} are the plane stress reduced elastic constants, defined as

$$C_{11} = C_{22} = \frac{E(z)}{(1 - \nu^2)} \tag{8a}$$

$$C_{12} = \nu C_{11} \tag{8b}$$

$$C_{44} = C_{55} = C_{66} = \frac{E(z)}{2(1+\nu)} \tag{8c}$$

If $\varepsilon_z \neq 0$ (thickness stretching), then C_{ij} are the three-dimensional elastic constants, given by

$$C_{11} = C_{22} = C_{33} = \frac{(1-\nu)E(z)}{(1-2\nu)(1+\nu)} \tag{9a}$$

$$C_{12} = C_{13} = C_{23} = \frac{E(z)}{(1-2\nu)(1+\nu)} \tag{9b}$$

$$C_{44} = C_{55} = C_{66} = \frac{E(z)}{2(1+\nu)} \tag{9c}$$

Lame's coefficients are:

$$\lambda(z) = \frac{\nu E(z)}{(1-2\nu)(1+\nu)}; \quad \mu(z) = G(z) = \frac{E(z)}{2(1+\nu)} \tag{10}$$

The module $E(z)$, $G(z)$ and the elastic coefficients C_{ij} vary through the thickness according to Eq. (3)

2.5 Governing equations

The governing equations of equilibrium can be derived by using the principle of virtual displacements. The principle of virtual work in the present case yields

$$\delta U + \delta V = 0 \tag{11}$$

Where δU is the variation of strain energy and δV is the variation of potential energy. The variation of strain energy of the plate is calculated by

$$\delta U = \int_{-h/2}^{h/2} \int_A (\sigma_x \delta\varepsilon_x + \sigma_y \delta\varepsilon_y + \sigma_z \delta\varepsilon_z + \sigma_{xy}\delta\gamma_{xy} + \sigma_{yz}\delta\gamma_{yz} + \sigma_{xz}\delta\gamma_{xz}).dA.dz \tag{12}$$

$$\begin{aligned} \delta U = \frac{1}{2}\int_A [& N_x \frac{\partial u_0}{\partial x} - M_x^b \frac{\partial^2 w_b}{\partial x^2} - M_x^s \frac{\partial^2 w_s}{\partial x^2} \\ & + N_y \frac{\partial v_0}{\partial y} - M_y^b \frac{\partial^2 w_b}{\partial y^2} - M_y^s \frac{\partial^2 w_s}{\partial y^2} + N_z w_z \\ & + N_{xy}\left(\frac{\partial u_0}{\partial y} + \frac{\partial v_0}{\partial x}\right) - 2M_{xy}^b \frac{\partial^2 w_b}{\partial x \partial y} - 2M_{xy}^s \frac{\partial^2 w_s}{\partial x \partial y} \\ & + S_x\left(\frac{\partial w_s}{\partial x} + \frac{\partial w_z}{\partial x}\right) + S_y\left(\frac{\partial w_s}{\partial y} + \frac{\partial w_z}{\partial y}\right)]dA \end{aligned} \tag{13}$$

Where A is the top surface and the stress resultants N; M, and Q are defined by

$$\begin{Bmatrix} N_x, & N_y, & N_{xy} \\ M_x^b, & M_y^b, & M_{xy}^b \\ M_x^s, & M_y^s, & M_{xy}^s \end{Bmatrix} = \int_{-h/2}^{h/2} (\sigma_x, \sigma_y, \sigma_{xy}) \begin{Bmatrix} 1 \\ z \\ f(z) \end{Bmatrix} dz \tag{14a}$$

$$N_z = \int_{-h/2}^{h/2} (\sigma_z) g'(z) dz \tag{14b}$$

$$(S_x, S_y) = \int_{-h/2}^{h/2} (\tau_{xz}, \tau_{yz}) g(z) dz \tag{14c}$$

Where

$$\begin{aligned} N_x = {} & A_{11}\frac{\partial u_0}{\partial x} + A_{12}\frac{\partial v_0}{\partial y} - B_{11}\frac{\partial^2 w_b}{\partial x^2} \\ & - B_{12}\frac{\partial^2 w_b}{\partial y^2} - B_{11}^s\frac{\partial^2 w_s}{\partial x^2} - B_{12}^s\frac{\partial^2 w_s}{\partial y^2} + L_{13} w_z \end{aligned} \tag{15a}$$

$$\begin{aligned} N_y = {} & A_{12}\frac{\partial u_0}{\partial x} + A_{22}\frac{\partial v_0}{\partial y} - B_{12}\frac{\partial^2 w_b}{\partial x^2} \\ & - B_{22}\frac{\partial^2 w_b}{\partial y^2} - B_{12}^s\frac{\partial^2 w_s}{\partial x^2} - B_{22}^s\frac{\partial^2 w_s}{\partial y^2} + L_{23} w_z \end{aligned} \tag{15b}$$

$$N_{xy} = A_{66}\left(\frac{\partial u_0}{\partial y} + \frac{\partial v_0}{\partial x}\right) - 2B_{66}\frac{\partial^2 w_b}{\partial x \partial y} - 2B_{66}^s\frac{\partial^2 w_s}{\partial x \partial y} \tag{15c}$$

$$\begin{aligned} M_x^b = {} & B_{11}\frac{\partial u_0}{\partial x} + B_{12}\frac{\partial v_0}{\partial y} - D_{11}\frac{\partial^2 w_b}{\partial x^2} \\ & - D_{12}\frac{\partial^2 w_b}{\partial y^2} - D_{11}^s\frac{\partial^2 w_s}{\partial x^2} - D_{12}^s\frac{\partial^2 w_s}{\partial y^2} + L_{13}^a w_z \end{aligned} \tag{15d}$$

$$\begin{aligned} M_y^b = {} & B_{12}\frac{\partial u_0}{\partial x} + B_{22}\frac{\partial v_0}{\partial y} - D_{12}\frac{\partial^2 w_b}{\partial x^2} \\ & - D_{22}\frac{\partial^2 w_b}{\partial y^2} - D_{12}^s\frac{\partial^2 w_s}{\partial x^2} - D_{22}^s\frac{\partial^2 w_s}{\partial y^2} + L_{23}^a w_z \end{aligned} \tag{15e}$$

$$M_{xy}^b = B_{66}\left(\frac{\partial u_0}{\partial y} + \frac{\partial v_0}{\partial x}\right) - 2D_{66}\frac{\partial^2 w_b}{\partial x \partial y} - 2D_{66}^s\frac{\partial^2 w_s}{\partial x \partial y} \tag{15f}$$

$$\begin{aligned} M_x^s = {} & B_{11}^s\frac{\partial u_0}{\partial x} + B_{12}^s\frac{\partial v_0}{\partial y} - D_{11}^s\frac{\partial^2 w_b}{\partial x^2} \\ & - D_{12}^s\frac{\partial^2 w_b}{\partial y^2} - H_{11}^s\frac{\partial^2 w_s}{\partial x^2} - H_{12}^s\frac{\partial^2 w_s}{\partial y^2} + R_{13} w_z \end{aligned} \tag{15g}$$

$$\begin{aligned} M_y^s = {} & B_{12}^s\frac{\partial u_0}{\partial x} + B_{22}^s\frac{\partial v_0}{\partial y} - D_{12}^s\frac{\partial^2 w_b}{\partial x^2} \\ & - D_{22}^s\frac{\partial^2 w_b}{\partial y^2} - H_{12}^s\frac{\partial^2 w_s}{\partial x^2} - H_{22}^s\frac{\partial^2 w_s}{\partial y^2} + R_{23} w_z \end{aligned} \tag{15h}$$

$$M_{xy}^s = B_{66}^s\left(\frac{\partial u_0}{\partial y} + \frac{\partial v_0}{\partial x}\right) - 2D_{66}^s\frac{\partial^2 w_b}{\partial x \partial y} - 2H_{66}^s\frac{\partial^2 w_s}{\partial x \partial y} \tag{15i}$$

$$\begin{aligned} N_z = {} & L_{13}\frac{\partial u_0}{\partial x} + L_{23}\frac{\partial v_0}{\partial y} - L_{13}^a\frac{\partial^2 w_b}{\partial x^2} \\ & - L_{23}^a\frac{\partial^2 w_b}{\partial y^2} - R_{13}\frac{\partial^2 w_s}{\partial x^2} - R_{23}\frac{\partial^2 w_s}{\partial y^2} + R_{33}^a w_z \end{aligned} \tag{15j}$$

$$S_x = A_{55}^s\left(\frac{\partial w_s}{\partial x} + \frac{\partial w_z}{\partial x}\right) \tag{15k}$$

$$S_y = A_{44}^s\left(\frac{\partial w_s}{\partial y} + \frac{\partial w_z}{\partial y}\right) \tag{15l}$$

Where A_{ij}, B_{ij}, etc., are the plate stiffness, defined by

$$\begin{Bmatrix} A_{11} & B_{11} & D_{11} & B_{11}^s & D_{11}^s & H_{11}^s \\ A_{12} & B_{12} & D_{12} & B_{12}^s & D_{12}^s & H_{12}^s \\ A_{66} & B_{66} & D_{66} & B_{66}^s & D_{66}^s & H_{66}^s \end{Bmatrix} = \sum_{k=1}^{3}\int_{h_k}^{h_{k+1}} \lambda(z)\left(1, z, z^2, f(z), z\, f(z), f^2(z)\right)\begin{Bmatrix} \frac{1-\nu}{\nu} \\ 1 \\ \frac{1-2\nu}{2\nu} \end{Bmatrix} dz \tag{16a}$$

And

$$\left(A_{22}, B_{22}, D_{22}, B_{22}^s, D_{22}^s, H_{22}^s\right) = \left(A_{11}, B_{11}, D_{11}, B_{11}^s, D_{11}^s, H_{11}^s\right) \tag{16b}$$

$$A_{44}^s = A_{55}^s = \sum_{k=1}^{3}\int_{h_k}^{h_{k+1}} \mu(z)(g(z))^2 dz \tag{16c}$$

$$\begin{Bmatrix} L \\ L^a \\ R \\ R^a \end{Bmatrix} = \sum_{k=1}^{3}\int_{h_k}^{h_{k+1}} \lambda(z) \begin{Bmatrix} 1 \\ z \\ f(z) \\ g'(z)\frac{1-\nu}{\nu} \end{Bmatrix} g'(z) dz \tag{16d}$$

The variation of potential energy of the applied loads can be expressed thus

$$\delta V = -\int_A q\left(\delta w_b + \delta w_s + g(z)\delta w_z\right) dA \tag{17}$$

Where q is the distributed transverse load. Substituting the expressions for δU and δV from Eqs. (12) and (17) into Eq. (11) and integrating by parts, and collecting the coefficients of δu_0; δv_0; δw_b; δw_s and δw_z, the following equilibrium equations of the plate are obtained

$$\delta\, u_0 : \; \frac{\partial N_x}{\partial x} + \frac{\partial N_{xy}}{\partial y} = 0 \tag{18a}$$

$$\delta\, v_0 : \; \frac{\partial N_{xy}}{\partial x} + \frac{\partial N_y}{\partial y} = 0 \tag{18b}$$

$$\delta\, w_b : \; \frac{\partial^2 M_x^b}{\partial x^2} + 2\frac{\partial^2 M_{xy}^b}{\partial x \partial y} + \frac{\partial^2 M_y^b}{\partial y^2} + q = 0 \tag{18c}$$

$$\delta\, w_s : \; \frac{\partial^2 M_x^s}{\partial x^2} + 2\frac{\partial^2 M_{xy}^s}{\partial x \partial y} + \frac{\partial^2 M_y^s}{\partial y^2} + \frac{\partial S_x}{\partial x} + \frac{\partial S_y}{\partial y} + q = 0 \tag{18d}$$

$$\delta w_z : \; \frac{\partial S_x}{\partial x} + \frac{\partial S_y}{\partial y} - N_z + g(z) q = 0 \tag{18e}$$

By substituting Eq. (6) into Eq. (7) and the subsequent results into Eq. (14), the stress resultants are readily obtained as

$$\begin{Bmatrix} N \\ M^b \\ M^s \end{Bmatrix} = \begin{bmatrix} A & B & B^s \\ A & D & D^s \\ B^s & D^s & H^s \end{bmatrix} \begin{Bmatrix} \varepsilon \\ k^b \\ k^s \end{Bmatrix} + \begin{Bmatrix} L \\ L^a \\ R \end{Bmatrix} \varepsilon_z^0, \tag{19a}$$

$$S = A^s \gamma, \tag{19b}$$

$$N_z = R^a w_z + L(\varepsilon_x^0 + \varepsilon_y^0) + L^a(k_x^b + k_y^b) + R(k_x^s + k_y^s) \tag{19c}$$

Where

$$N = \{N_x, N_y, N_{xy}\}, \quad M^b = \{M_x^b, M_y^b, M_{xy}^b\}, \quad M^s = \{M_x^s, M_y^s, M_{xy}^s\}, \tag{20a}$$

$$\varepsilon = \{\varepsilon_x^0, \varepsilon_y^0, \gamma_{xy}^0\}, \quad k^b = \{k_x^b, k_y^b, k_{xy}^b\}, \quad k^s = \{k_x^s, k_y^s, k_{xy}^s\}, \tag{20b}$$

$$A = \begin{bmatrix} A_{11} & A_{12} & 0 \\ A_{12} & A_{22} & 0 \\ 0 & 0 & A_{66} \end{bmatrix}, \quad B = \begin{bmatrix} B_{11} & B_{12} & 0 \\ B_{12} & B_{22} & 0 \\ 0 & 0 & B_{66} \end{bmatrix}, \quad D = \begin{bmatrix} D_{11} & D_{12} & 0 \\ D_{12} & D_{22} & 0 \\ 0 & 0 & D_{66} \end{bmatrix}, \tag{20c}$$

$$B^s = \begin{bmatrix} B_{11}^s & B_{12}^s & 0 \\ B_{12}^s & B_{22}^s & 0 \\ 0 & 0 & B_{66}^s \end{bmatrix}, \quad D^s = \begin{bmatrix} D_{11}^s & D_{12}^s & 0 \\ D_{12}^s & D_{22}^s & 0 \\ 0 & 0 & D_{66}^s \end{bmatrix}, \quad H^s = \begin{bmatrix} H_{11}^s & H_{12}^s & 0 \\ H_{12}^s & H_{22}^s & 0 \\ 0 & 0 & H_{66}^s \end{bmatrix}, \tag{20d}$$

$$S = \{S_x, S_y\}, \quad \gamma = \{\gamma_{xz}, \gamma_{yz}\}, \quad A^s = \begin{bmatrix} A_{44}^s & 0 \\ 0 & A_{55}^s \end{bmatrix} \tag{20e}$$

Equilibrium equations in terms of displacements

Introducing Eq. (20) into Eq. (18), the equilibrium equations can be expressed in terms of displacements (δu_0; δv_0; δw_b; δw_s and δw_z,) and the appropriate equations take the form

$$\begin{aligned} & A_{11}\frac{\partial^2 u_0}{\partial x^2} + A_{66}\frac{\partial^2 u_0}{\partial y^2} + (A_{12}+A_{66})\frac{\partial^2 v_0}{\partial x \partial y} - B_{11}\frac{\partial^3 w_b}{\partial x^3} \\ & -(B_{12}+2B_{66})\frac{\partial^3 w_b}{\partial x \partial y^2} - (B_{12}^s + 2B_{66}^s)\frac{\partial^3 w_s}{\partial x \partial y^2} \\ & - B_{11}^s\frac{\partial^3 w_s}{\partial x^3} + L_{13}\frac{\partial w_z}{\partial x} = 0 \end{aligned} \tag{21a}$$

$$\begin{aligned} & A_{22}\frac{\partial^2 v_0}{\partial y^2} + A_{66}\frac{\partial^2 v_0}{\partial x^2} + (A_{12}+A_{66})\frac{\partial^2 u_0}{\partial x \partial y} - B_{22}\frac{\partial^3 w_b}{\partial y^3} \\ & -(B_{12}+2B_{66})\frac{\partial^3 w_b}{\partial x^2 \partial y} - (B_{12}^s + 2B_{66}^s)\frac{\partial^3 w_s}{\partial x^2 \partial y} \\ & - B_{22}^s\frac{\partial^3 w_s}{\partial y^3} + L_{23}\frac{\partial w_z}{\partial y} = 0 \end{aligned} \tag{21b}$$

Table 1 Comparison of the Dimensionless stress and deflection of sandwich square plates embedding an FGM (Al/ Al_2O_3) core with a polynomial material law subjected to sinusoidal distributed load

p	Theory	$\bar{w}(a/2,b/2,0)$			$\bar{\sigma}_{xz}(0,b/2,h/6)$			$\bar{\sigma}_{xx}(0,b/2,h/3)$	
		a/*h*=4	*a*/*h*=10	*a*/*h*=100	*a*/*h*=4	*a*/*h*=10	*a*/*h*=100	*a*/*h*=4	*a*/*h*=100
1	Present Model 1- $\varepsilon_z \neq 0$	0.7276	0.6060	0.5827	0.2713	0.2724	0.2726	0.6131	15.2932
	Present Model 2- $\varepsilon_z \neq 0$	0.7263	0.6050	0.5817	0.2718	0.2728	0.2730	0.6044	14.9927
	Mantari (2014)- $\varepsilon_z \neq 0$	0.728	0.606	0.583	0.271	0.272	0.273	0.613	15.290
	Thai and Kim (2013)- $\varepsilon_z = 0$	0.725	0.604	0.581	0.272	0.273	0.273	0.601	14.861
	Neves, Ferreira *et al.* - Quasi-3D (2012)	0.742	0.631	0.609	0.274	0.279	0.279	-	-
	Tounsi, Menaa *et al.* -FSDT- $\varepsilon_z = 0$ - (2012)	0.774	0.634	0.607	0.246	0.246	0.246	0.697	17.344
4	Present Model 1- $\varepsilon_z \neq 0$	1.0164	0.7815	0.7366	0.2596	0.2610	0.2613	0.4606	12.1058
	Present Model 2- $\varepsilon_z \neq 0$	1.0170	0.7805	0.7351	0.2633	0.2649	0.2652	0.4480	11.7222
	Mantari (2014)- $\varepsilon_z \neq 0$	1.016	0.782	0.737	0.260	0.261	0.261	-	-
	Thai and Kim (2013)- $\varepsilon_z = 0$	1.017	0.780	0.734	0.265	0.266	0.267	-	-
	Neves, Ferreira *et al.* - Quasi-3D (2012)	1.039	0.820	0.778	0.272	0.278	0.279	-	-
	Tounsi, Menaa *et al.* -FSDT- $\varepsilon_z = 0$- (2012)	1029	0.819	0780	0.188	0.188	0.188	-	-
10	Present Model 1- $\varepsilon_z \neq 0$	1.1535	0.8316	0.7701	0.1900	0.1912	0.1914	0.3234	9.0206
	Present Model 2- $\varepsilon_z \neq 0$	1.1562	0.8321	0.7700	0.1930	0.1945	0.1947	0.3097	8.6357
	Mantari (2014)- $\varepsilon_z \neq 0$	1.153	0.832	0.770	0.190	0.191	0.191	0.323	9.015
	Thai and Kim (2013)- $\varepsilon_z \neq 0$	1.157	0.832	0.769	0.194	0.196	0.196	0.304	8.458
	Neves, Ferreira *et al.* - Quasi-3D (2012)	1.178	0.865	0.805	0.202	0.206	0.206	-	-
	Tounsi, Menaa *et al.* -FSDT- $\varepsilon_z = 0$- (2012)	1.111	0.856	0.808	0.123	0.123	0.123	0.420	10.495

$$
\begin{aligned}
& B_{11}\frac{\partial^3 u_0}{\partial x^3} + (B_{12}+2B_{66})\frac{\partial^3 u_0}{\partial x \partial y^2} + \\
& (B_{12}+2B_{66})\frac{\partial^3 v_0}{\partial x^2 \partial y} + B_{22}\frac{\partial^3 v_0}{\partial y^3} - D_{11}\frac{\partial^4 w_b}{\partial x^4} \\
& -2(D_{12}+2D_{66})\frac{\partial^4 w_b}{\partial x^2 \partial y^2} - D_{22}\frac{\partial^4 w_b}{\partial y^4} - D_{11}^s\frac{\partial^4 w_s}{\partial x^4} \\
& -2(D_{12}^s+2D_{66}^s)\frac{\partial^4 w_s}{\partial x^2 \partial y^2} - D_{22}^s\frac{\partial^4 w_s}{\partial y^4} \\
& + L_{13}^a\frac{\partial^2 w_z}{\partial x^2} + L_{23}^a\frac{\partial^2 w_z}{\partial y^2} + q = 0
\end{aligned}
\tag{21c}
$$

$$
\begin{aligned}
& B_{11}^s\frac{\partial^3 u_0}{\partial x^3} + (B_{12}^s+2B_{66}^s)\frac{\partial^3 u_0}{\partial x \partial y^2} \\
& + (B_{12}^s+2B_{66}^s)\frac{\partial^3 v_0}{\partial x^2 \partial y} + B_{22}^s\frac{\partial^3 v_0}{\partial y^3} - D_{11}^s\frac{\partial^4 w_b}{\partial x^4} \\
& -2(D_{12}^s+2D_{66}^s)\frac{\partial^4 w_b}{\partial x^2 \partial y^2} - D_{22}^s\frac{\partial^4 w_b}{\partial y^4} \\
& - H_{11}^s\frac{\partial^4 w_s}{\partial x^4} - 2(H_{12}^s+2H_{66}^s)\frac{\partial^4 w_s}{\partial x^2 \partial y^2} \\
& - H_{22}^s\frac{\partial^4 w_s}{\partial y^4} + A_{55}^s\frac{\partial^2 w_s}{\partial x^2} + A_{44}^s\frac{\partial^2 w_s}{\partial y^2} + \\
& + (R_{13}+A_{55}^s)\frac{\partial^2 w_z}{\partial x^2} + (R_{23}+A_{44}^s)\frac{\partial^2 w_z}{\partial y^2} + q = 0
\end{aligned}
\tag{21d}
$$

$$
+ (R_{13}+A_{55}^s)\frac{\partial^2 w_z}{\partial x^2} + (R_{23}+A_{44}^s)\frac{\partial^2 w_z}{\partial y^2} + q = 0
$$

$$
\begin{aligned}
& - L_{13}\frac{\partial u_0}{\partial x} - L_{23}\frac{\partial v_0}{\partial y} + L_{13}^a\frac{\partial^2 w_b}{\partial x^2} + L_{23}^a\frac{\partial^2 w_b}{\partial y^2} \\
& + (R_{13}+A_{55}^s)\frac{\partial^2 w_s}{\partial x^2} + (R_{23}+A_{44}^s)\frac{\partial^2 w_s}{\partial y^2} \\
& + A_{55}^s\frac{\partial^2 w_z}{\partial x^2} + A_{44}^s\frac{\partial^2 w_z}{\partial y^2} - R_{33}^a w_z + gq = 0
\end{aligned}
\tag{21e}
$$

2.6 Analytical solutions

Consider a simply supported rectangular sandwich plate with length a and width b under transverse load q. Based on Navier solution method, the following expansions of displacements (u_0; v_0, w_b; w_s; w_z) are assumed as

$$
\begin{aligned}
u_0(x,y) &= \sum_{m=1}^{\infty}\sum_{n=1}^{\infty} U_{mn}\cos(\lambda x)\sin(\mu y) \\
v_0(x,y) &= \sum_{m=1}^{\infty}\sum_{n=1}^{\infty} V_{mn}\sin(\lambda x)\cos(\mu y) \\
w_b(x,y) &= \sum_{m=1}^{\infty}\sum_{n=1}^{\infty} W_{bmn}\sin(\lambda x)\sin(\mu y) \\
w_s(x,y) &= \sum_{m=1}^{\infty}\sum_{n=1}^{\infty} W_{smn}\sin(\lambda x)\sin(\mu y) \\
w_z(x,y) &= \sum_{m=1}^{\infty}\sum_{n=1}^{\infty} W_{zmn}\sin(\lambda x)\sin(\mu y)
\end{aligned}
\tag{22}
$$

Where U_{mn},V_{mn}, W_{bmn}, W_{smn} and W_{zmn} unknown parameters must be determined, and $\lambda = \frac{m\pi}{a}$ and $\mu = \frac{n\pi}{b}$.

The transverse load q is also expanded in the double-Fourier sine series as follows

Table 2 Comparisons of dimensionless deflection $\overline{w}$ of simply supported of sandwich square power-law FGM (Al/ ZrO_2) plates with other theories (*a/b*=1, *a/h*=10)

p	Théorie	ε_z	$\overline{w}$				
			1-0-1	2-1-2	1-1-1	2-2-1	1-2-1
0	Present Model 1	$\varepsilon_z \neq 0$	0.19457	0.19457	0.19457	0.19457	0.19457
	Present Model 2	$\varepsilon_z \neq 0$	0.19487	0.19487	0.19487	0.19487	0.19487
	Model Daouadji, Tounsi *et al*. (2013)	$\varepsilon_z \neq 0$	0.19606	0.19606	0.19606	0.19606	0.19606
	Model Reddy (1984)	$\varepsilon_z = 0$	0.19605	0.19605	0.19605	0.19605	0.19605
1	Present Model 1	$\varepsilon_z \neq 0$	0.32096	0.30383	0.28963	0.27834	0.26879
	Present Model 2	$\varepsilon_z \neq 0$	0.32149	0.30431	0.29007	0.27876	0.26916
	Model Daouadji, Tounsi *et al*. (2013)	$\varepsilon_z = 0$	0.32358	0.30631	0.29199	0.28085	0.27094
	Model Reddy (1984)	$\varepsilon_z = 0$	0.32349	0.30624	0.29194	0.28082	0.27093
2	Present Model 1	$\varepsilon_z \neq 0$	0.37028	0.34939	0.33013	0.31303	0.30017
	Present Model 2	$\varepsilon_z \neq 0$	0.37096	0.35002	0.33069	0.31356	0.30061
	Model Daouadji, Tounsi *et al*. (2013)	$\varepsilon_z = 0$	0.37334	0.35231	0.33288	0.31616	0.30263
	Model Reddy (1984)	$\varepsilon_z = 0$	0.37319	0.35218	0.33284	0.31611	0.30260
5	Present Model 1	$\varepsilon_z \neq 0$	0.40595	0.38855	0.36832	0.34576	0.33201
	Present Model 2	$\varepsilon_z \neq 0$	0.40672	0.38933	0.36903	0.34648	0.33256
	Model Daouadji, Tounsi *et al*. (2013)	$\varepsilon_z = 0$	0.40927	0.39182	0.37144	0.34960	0.33480
	Model Reddy (1984)	$\varepsilon_z = 0$	0.40905	0.39160	0.37128	0.34950	0.33474
10	Present Model 1	$\varepsilon_z \neq 0$	0.41412	0.40093	0.37809	0.35803	0.34532
	Present Model 2	$\varepsilon_z \neq 0$	0.41515	0.40153	0.38303	0.35883	0.34592
	Model Daouadji, Tounsi *et al*. (2013)	$\varepsilon_z = 0$	0.41772	0.40407	0.38551	0.36212	0.34823
	Model Reddy (1984)	$\varepsilon_z = 0$	0.41750	0.40376	0.38490	0.34916	0.34119

$$q(x,y)=\sum_{m=1}^{\infty}\sum_{n=1}^{\infty}Q_{mn}\sin(\lambda x)\sin(\mu y) \tag{23}$$

The coefficients Qmn are given below for some typical loads

$$Q_{mn}=\frac{4}{ab}\int_0^a\int_0^b q(x,y)\sin(\lambda x)\sin(\mu y)\,dx\,dy$$

$$\begin{cases} Q_{mn}=q_0 \\ Q_{mn}=\dfrac{16q_0}{mn\pi^2} \end{cases} \tag{24}$$

Substituting from Eq. (22) into Eq. (21), we obtain the following operator equation

$$\begin{bmatrix} a_{11} & a_{12} & a_{13} & a_{14} & a_{15} \\ a_{12} & a_{22} & a_{23} & a_{24} & a_{25} \\ a_{13} & a_{23} & a_{33} & a_{34} & a_{35} \\ a_{14} & a_{24} & a_{34} & a_{44} & a_{45} \\ a_{15} & a_{25} & a_{35} & a_{45} & a_{55} \end{bmatrix}\begin{Bmatrix} U_{mn} \\ V_{mn} \\ W_{bmn} \\ W_{smn} \\ W_{zmn} \end{Bmatrix}=\begin{Bmatrix} 0 \\ 0 \\ Q_{mn} \\ Q_{mn} \\ 0 \end{Bmatrix} \tag{25}$$

Where

$$a_{11}=A_{11}\lambda^2+A_{66}\mu^2\ ;\quad a_{12}=\lambda\mu(A_{12}+A_{66});$$
$$a_{13}=-\lambda[B_{11}\lambda^2+(B_{12}+2B_{66})\mu^2]$$
$$a_{14}=-\lambda[B^s_{11}\lambda^2+(B^s_{12}+2B^s_{66})\mu^2];\quad a_{15}=L_{13}\lambda;$$

$$\begin{aligned} &a_{22}=A_{66}\lambda^2+A_{22}\mu^2 \\ &a_{23}=-\mu[B_{22}\mu^2+(B_{12}+2B_{66})\lambda^2]\ ; \\ &a_{24}=-\mu[B^s_{22}\mu^2+(B^s_{12}+2B^s_{66})\lambda^2];\quad a_{25}=L_{23}\mu \\ &a_{35}=L^a_{13}\lambda^2+L^a_{23}\mu^2\ ; \\ &a_{33}=D_{11}\lambda^4+2(D_{12}+2D_{66})\lambda^2\mu^2+D_{22}\mu^4\ ; \\ &a_{34}=D^s_{11}\lambda^4+2(D^s_{12}+2D^s_{66})\lambda^2\mu^2+D^s_{22}\mu^4 \\ &a_{44}=H^s_{11}\lambda^4+2(H^s_{12}+2H^s_{66})\lambda^2\mu^2+H^s_{22}\mu^4+A^s_{55}\lambda^2+A^s_{44}\mu^2; \\ &a_{45}=(R_{13}+A^s_{55})\lambda^2+(R_{23}+A^s_{44})\mu^2\ ; \\ &a_{55}=A^s_{55}\lambda^2+A^s_{44}\mu^2+R^a_{33} \end{aligned} \tag{26}$$

3. Numerical results and discussions

To illustrate the proposed approach, a simple quasi-3D higher order shear and normal deformation theory with stretching effect for composite sandwich plates is suggested for investigation. Navier solutions for bending analysis of FGM plates are presented by solving Eq. (25). In this section, the analysis is conducted for two combinations of metal and ceramic. The first set of materials chosen is aluminium and alumina. The second combination of materials consisted of aluminium and zirconia. The material

Table 3 Comparisons of dimensionless axial stress $\bar{\sigma}_x$ of simply supported of sandwich square power-law FGM (Al/ ZrO_2) plates with other theories (a/b=1, a/h=5)

p	Théorie	ε_z	$\bar{\sigma}_x$				
			1-0-1	2-1-2	1-1-1	2-2-1	1-2-1
0	Present Model 1	$\varepsilon_z \neq 0$	2.17149	2.17149	2.17149	2.17149	2.17149
	Present Model 2	$\varepsilon_z \neq 0$	2.09913	2.09913	2.09913	2.09913	2.09913
	Model Daouadji, Tounsi *et al*. (2013)	$\varepsilon_z = 0$	2.04985	2.04985	2.04985	2.04985	2.04985
	Model Reddy (1984)	$\varepsilon_z = 0$	2.05452	2.05452	2.05452	2.05452	2.05452
1	Present Model 1	$\varepsilon_z \neq 0$	1.95497	1.85357	1.76916	1.62906	1.64362
	Present Model 2	$\varepsilon_z \neq 0$	1.82413	1.72791	1.64816	1.51308	1.53055
	Model Daouadji, Tounsi *et al*. (2013)	$\varepsilon_z = 0$	1.57923	1.49587	1.42617	1.32062	1.32309
	Model Reddy (1984)	$\varepsilon_z = 0$	1.58204	1.49859	1.42892	1.32342	1.32590
2	Present Model 1	$\varepsilon_z \neq 0$	2.24963	2.12892	2.01678	1.81178	1.83896
	Present Model 2	$\varepsilon_z \neq 0$	2.10177	1.98540	1.87804	1.67955	1.71005
	Model Daouadji, Tounsi *et al*. (2013)	$\varepsilon_z = 0$	1.82167	1.72144	1.62748	1.47095	1.47988
	Model Reddy (1984)	$\varepsilon_z = 0$	1.82450	1.72412	1.63025	1.47387	1.48283
5	Present Model 1	$\varepsilon_z \neq 0$	2.45428	2.35697	2.24326	1.98085	2.03306
	Present Model 2	$\varepsilon_z \neq 0$	2.29951	2.20357	2.09209	1.83534	1.89036
	Model Daouadji, Tounsi *et al*. (2013)	$\varepsilon_z = 0$	1.99272	1.91302	1.81580	1.61181	1.63814
	Model Reddy (1984)	$\varepsilon_z = 0$	1.99567	1.91547	1.81838	1.61477	1.64108
10	Present Model 1	$\varepsilon_z \neq 0$	2.50188	2.41351	2.23916	2.04386	2.11217
	Present Model 2	$\varepsilon_z \neq 0$	2.34582	2.27035	2.16923	1.89412	1.96490
	Model Daouadji, Tounsi *et al*. (2013)	$\varepsilon_z = 0$	2.03036	1.97126	1.88377	1.66480	1.70383
	Model Reddy (1984)	$\varepsilon_z = 0$	2.03360	1.97313	1.88147	1.66979	1.64851

Table 4 Comparisons of dimensionless transverse shear stress $\bar{\tau}_{xz}$ of simply supported of sandwich square power-law FGM (Al/ ZrO_2) plates with other theories (a/b=1, a/h=5)

p	Théorie	ε_z	$\bar{\tau}_{xz}$				
			1-0-1	2-1-2	1-1-1	2-2-1	1-2-1
0	Present Model 1	$\varepsilon_z \neq 0$	0.24300	0.24300	0.24300	0.24300	0.24300
	Present Model 2	$\varepsilon_z \neq 0$	0.23805	0.23805	0.23805	0.23805	0.23805
	Model Daouadji, Tounsi *et al*. (2013)	$\varepsilon_z = 0$	0.23857	0.23857	0.23857	0.23857	0.23857
	Model Reddy (1984)	$\varepsilon_z = 0$	0.24918	0.24918	0.24918	0.24918	0.24918
1	Present Model 1	$\varepsilon_z \neq 0$	0.29604	0.27490	0.26521	0.26382	0.25703
	Present Model 2	$\varepsilon_z \neq 0$	0.29157	0.27063	0.26077	0.25910	0.25218
	Model Daouadji, Tounsi *et al*. (2013)	$\varepsilon_z = 0$	0.29202	0.27104	0.26116	0.25950	0.25258
	Model Reddy (1984)	$\varepsilon_z = 0$	0.29907	0.27774	0.26809	0.26680	0.26004
2	Present Model 1	$\varepsilon_z \neq 0$	0.32982	0.29157	0.27537	0.27339	0.26253
	Present Model 2	$\varepsilon_z \neq 0$	0.32572	0.28796	0.27148	0.26900	0.25796
	Model Daouadji, Tounsi *et al*. (2013)	$\varepsilon_z = 0$	0.32622	0.28838	0.27187	0.26939	0.25833
	Model Reddy (1984)	$\varepsilon_z = 0$	0.33285	0.29422	0.27807	0.27627	0.26543
5	Present Model 1	$\varepsilon_z \neq 0$	0.39022	0.31688	0.28906	0.28620	0.26878
	Present Model 2	$\varepsilon_z \neq 0$	0.38570	0.31409	0.28602	0.28225	0.26474
	Model Daouadji, Tounsi *et al*. (2013)	$\varepsilon_z = 0$	0.38634	0.31454	0.28642	0.28265	0.26512
	Model Reddy (1984)	$\varepsilon_z = 0$	0.39370	0.31930	0.29150	0.28895	0.27153
10	Present Model 1	$\varepsilon_z \neq 0$	0.43703	0.33454	0.29789	0.29421	0.27227
	Present Model 2	$\varepsilon_z \neq 0$	0.43127	0.33194	0.29525	0.29042	0.26856
	Model Daouadji, Tounsi *et al*. (2013)	$\varepsilon_z = 0$	0.43206	0.33242	0.29083	0.29083	0.26894
	Model Reddy (1984)	$\varepsilon_z = 0$	0.44147	0.33644	0.29529	0.29671	0.27676

Table 5 Effect of aspect ratio *a/b* on the dimensionless deflection of the FGM (Al/ ZrO_2) sandwich plates (P=2, a/h=10)

	Théorie	ε_z	$\bar{w}$				
			a/b=1/3	a/b=1/2	a/b=1	a/b=3/2	a/b=2
1-0-1	Present Model 1	$\varepsilon_z \neq 0$	1.18240	0.93638	0.37028	0.14306	0.06211
	Present Model 2	$\varepsilon_z \neq 0$	0.18450	0.93805	0.37096	0.14333	0.06224
	Model Daouadji, Tounsi *et al*. (2013)	$\varepsilon_z = 0$	1.18877	0.94185	0.37335	0.14481	0.06321
	Model Reddy (1984)	$\varepsilon_z = 0$	1.18849	0.94160	0.37319	0.14472	0.06315
2-1-2	Present Model 1	$\varepsilon_z \neq 0$	1.11684	0.88432	0.34939	0.13480	0.05842
	Present Model 2	$\varepsilon_z \neq 0$	1.11882	0.88589	0.35002	0.13505	0.05852
	Model Daouadji, Tounsi *et al*. (2013)	$\varepsilon_z = 0$	1.12293	0.88954	0.35231	0.13647	0.05946
	Model Reddy (1984)	$\varepsilon_z = 0$	1.12269	0.88933	0.35218	0.13639	0.05941
1-1-1	Present Model 1	$\varepsilon_z \neq 0$	1.05521	0.83553	0.33013	0.12738	0.05521
	Present Model 2	$\varepsilon_z \neq 0$	1.05702	0.83696	0.33069	0.12759	0.05530
	Model Daouadji, Tounsi *et al*. (2013)	$\varepsilon_z = 0$	1.06096	0.84046	0.33288	0.12895	0.05619
	Model Reddy (1984)	$\varepsilon_z = 0$	1.06080	0.84032	0.33280	0.12890	0.05615
2-2-1	Present Model 1	$\varepsilon_z \neq 0$	0.99974	0.79171	0.31303	0.12092	0.05248
	Present Model 2	$\varepsilon_z \neq 0$	1.00150	0.79309	0.31356	0.12111	0.05256
	Model Daouadji, Tounsi *et al*. (2013)	$\varepsilon_z = 0$	1.00694	0.79776	0.31617	0.12260	0.05349
	Model Reddy (1984)	$\varepsilon_z = 0$	1.00683	0.79767	0.31611	0.12256	0.05347
1-2-1	Present Model 1	$\varepsilon_z \neq 0$	0.95860	0.75914	0.30017	0.11596	0.05034
	Present Model 2	$\varepsilon_z \neq 0$	0.96009	0.76031	0.30061	0.11611	0.05040
	Model Daouadji, Tounsi *et al*. (2013)	$\varepsilon_z = 0$	0.96371	0.76353	0.30263	0.11737	0.05122
	Model Reddy (1984)	$\varepsilon_z = 0$	0.96366	0.76348	0.30260	0.1735	0.05121

properties are as follow:

Ceramic (Zirconia, ZrO_2): E_c= 151 GPa; ν=0.3.

Ceramic (Alumina, Al_2O_3): E_c= 380 GPa; ν=0.3.

Metal (Aluminium, Al): E_m= 70 GPa; ν=0.3.

Numerical results are presented in terms of non-dimensional stresses and deflection. The various nondimensional parameters used are

$$\bar{W} = \frac{10hE_0}{q_0 a^2} W\left(\frac{a}{2},\frac{b}{2}\right), \quad \bar{\sigma}_x = \frac{10.h^2}{q_0 a^2}\sigma_x\left(\frac{a}{2},\frac{b}{2},\frac{h}{2}\right),$$

$$\bar{\tau}_{xz} = \frac{h}{q_0 a}\tau_{xz}\left(0,\frac{b}{2},0\right).$$

Numerical results are presented in tabulated in Tables 1-5 and graphically plotted in Figs. 3-11 using the present model (Present model 1). The non-dimensional transverse displacement $\bar{w}(a/2,b/2,0)$, in-plane normal stresses $\bar{\sigma}_{xz}(0,b/2,h/6)$, and transverse shear stress $\bar{\sigma}_{xx}(0,b/2,h/3)$ are presented in Table 1. The present results are compared by accurate quasi-3D higher order shear deformation theory by Neves, Ferreira *et al.* (2012). The last group of theories were built based on previous authors experience on meshless numerical method and the CUF within a remarkable joint work between the authors (Carrera 2011). Displacement and transverse shear stresses results are in good agreement with the referential solution (Tounsi 2012, Neves 2012, Mantari 2014, Thai 2013). Neves which use 9-unknowns to model the displacement field. The Neves theory in (Neves 2012) also use 9-unknowns but the results of transverse shear stresses are far from the referential solution. This theory could be perhaps optimized in order to select a proper shear strain functions. In the case of normal stresses, these presents theories produces results that are closer to the referential solution (Neves 2012) than the model presented by Thai and Kim (2013). In general, we can say that this theory is more effective, as long as the results are comparable to the models presented. Analytical study emerged the numerical results of simply supported square power-law FGM (Al/ ZrO2) plates are presented in Tables 2, 3 and 4. These Tables consider the case of homogeneous hardcore in which the Young's modulus of layer 1 ZrO2 are *Ec*=51 GPa at the top face and *Em*=70 GPa at the bottom face Al. The results are considered for P=0, 1, 2, 5, and 10 and different types of sandwich square plates. It can be seen that the results obtained by Hassaine Daouadji el al (ε_z=0) (2013); Reddy (ε_z=0) (1984) and these presents theories ($\varepsilon_z \neq 0$) are signified clearly the stretching effect. The comparisons of the maximum deflections are given in Table 5 for FGM (Al/ ZrO2) sandwich plate with homogeneous hardcore and with volume fraction indices P=2. We can say that in the light of the results obtained that the stretching effect is very well demonstrated; object of our research. In addition, the deflection will decreases as the aspect ratio *a/b* increases.

The second part of the results will be devoted to the graphical presentation which Figs. 3-8 present some numerical results of simply supported square power-law

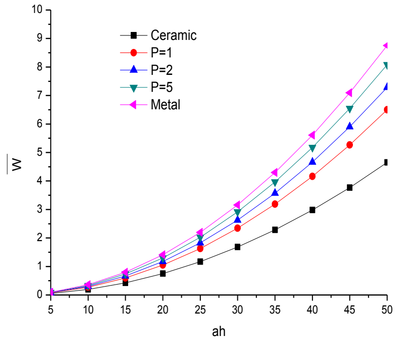

(a) The 1-2-1 FGM sandwich plate

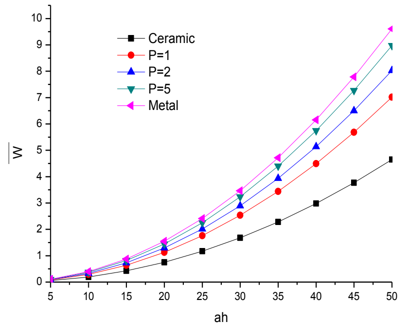

(b) The 1-1-1 FGM sandwich plate

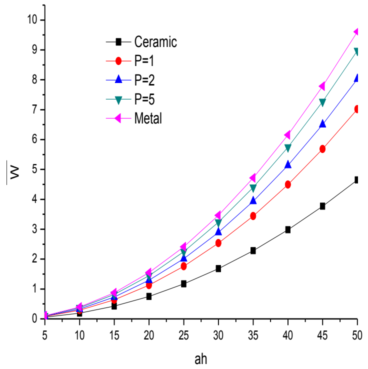

(c) The 2-1-2 FGM sandwich plate

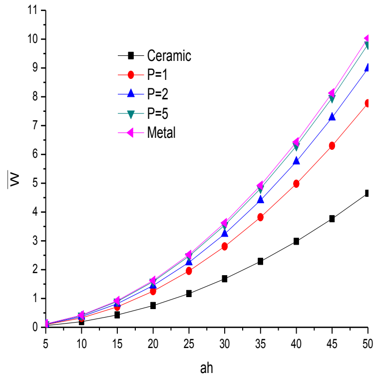

(d) The 1-0-1 FGM sandwich plate

Fig. 3 Dimensionless center deflection $\overline{w}$ as a function of side-to-thickness ratio *a/h* of FGM sandwich (Al/ ZrO_2) plate with homogeneous hardcore for various values of *P* and different types of sandwich plates
- Present model 1 –

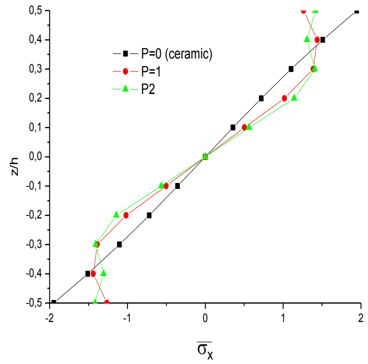

(a) The 1-2-1 FGM sandwich plate

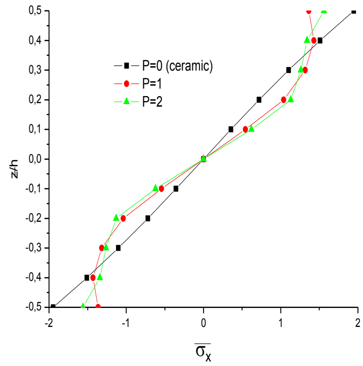

(b) The 1-1-1 FGM sandwich plate

Fig. 4 Variation of normal stress $\bar{\sigma}_x$ through plate thickness of FGM sandwich plate (Al/ ZrO_2) with homogeneous hardcore for various values of *P* and different types of sandwich plates (*a/h*=10)
- Present model 1 -

FGM (Al/ ZrO_2) plates using the present model 1 (Hyperbolic Shear Deformation Theory). Fig. 3 shows the variation of the center deflection with side to-thickness ratio a/h for different type of FGM (Al/ ZrO_2) symmetric plates with a homogeneous hardcore. The deflection of the Aluminium plate is found to be the largest magnitude and that of the ceramic (ZrO_2) plate of the smallest magnitude. The deflections increase when *a/h*≥10. All the plates with intermediate properties undergo corresponding intermediate values of center deflection. Which can be classified as very logical because the Aluminium plate is the one with the lowest stiffness and the ceramic (ZrO_2) plate is the one with the highest stiffness. The axial stress $\bar{\sigma}_x$ through-the-thickness of the plate with a homogeneous hardcore (Fig. 4). Under the application of the sinusoidal loading, the stresses are tensile at the top surface and compressive at the bottom surface. The homogeneous ceramic (ZrO_2) plate yields the maximum compressive (tensile) stress at the bottom (top) surface. The shape of the curves shows that the stress profile for plate made of pure material ZrO_2 (ceramic) changes linearly through the thickness. However, the axial stress variation is not linear for FGM plate. We have plotted

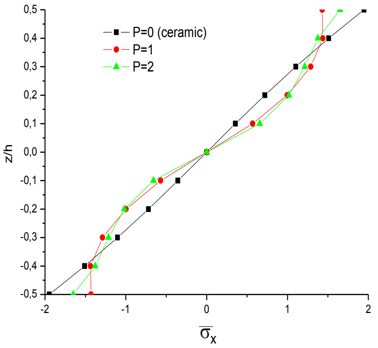

(c) The 2-1-2 FGM sandwich plate

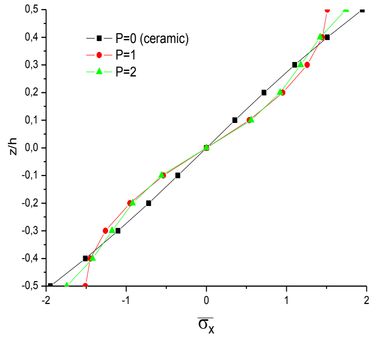

(d) The 1-0-1 FGM sandwich plate

Fig. 4 Continued

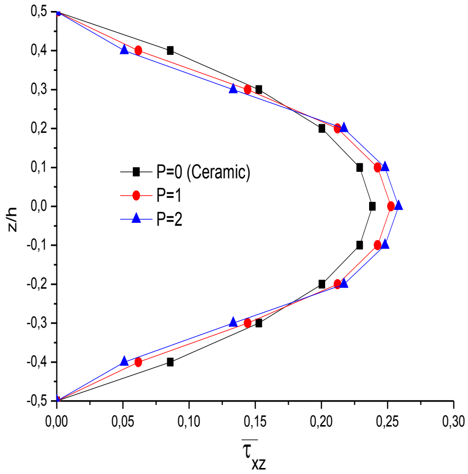

(a) The 1-2-1 FGM sandwich plate

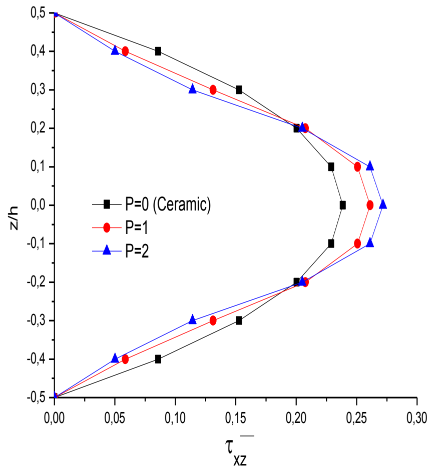

(b) The 1-1-1 FGM sandwich plate

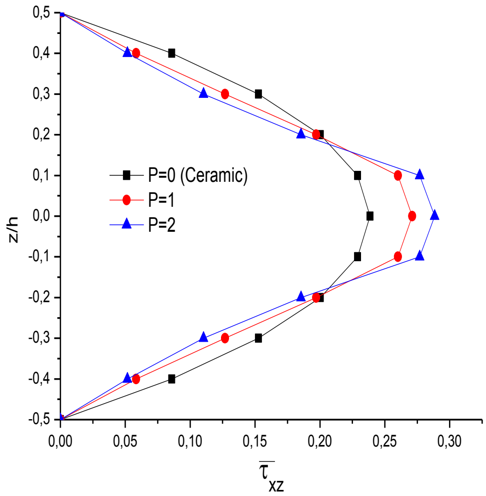

(c) The 2-1-2 FGM sandwich plate

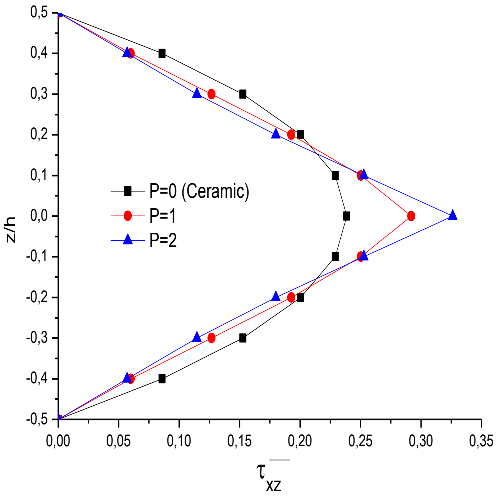

(d) The 1-0-1 FGM sandwich plate

Fig. 5 Variation of transverse shear stress $\bar{\tau}_{xz}$ through plate thickness of FGM sandwich (Al/ ZrO_2) plate with homogeneous hardcore for various values of *P* and different types of sandwich plates (*a*/*h*=10)
- Present model 1 -

the transverse shear stress $\bar{\tau}_{xz}$ through-the-thickness of the plate in Fig. 5 with a homogeneous hardcore. The maximum value occurs at a point on the mid-plane of the plate and its magnitude for FGM (Al/ ZrO_2) plate is larger than that for homogeneous ceramic plate (ZrO_2). The variation of the center deflection with side-to-thickness ratio for different type of FGM symmetric plates with a homogeneous soft core in which the Young's modulus is presented in Fig. 6. Contrary to the case of homogeneous hard core, it can be observed that for FGM (Al/ ZrO_2) plates

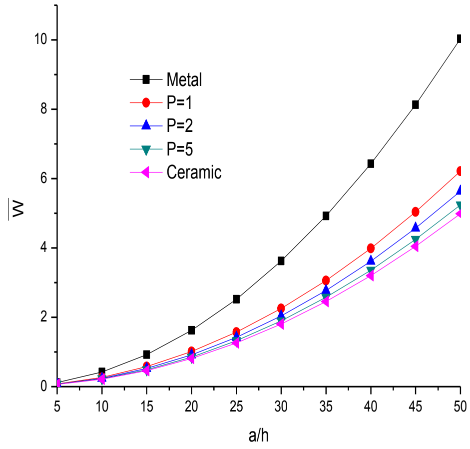

(a) The 1-2-1 FGM sandwich plate

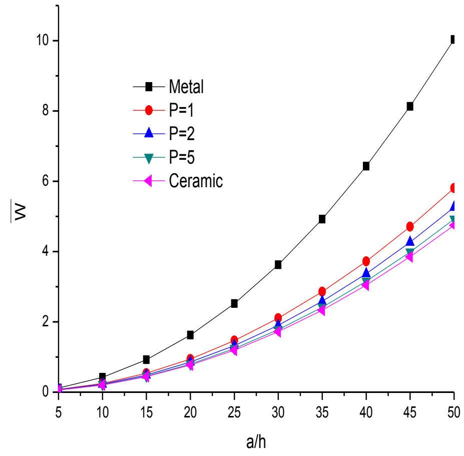

(b) The 1-1-1 FGM sandwich plate

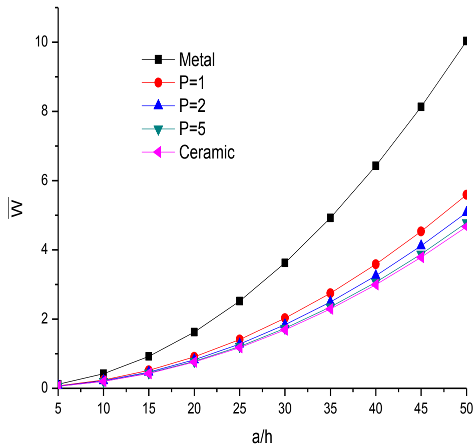

(c) The 2-1-2 FGM sandwich plate

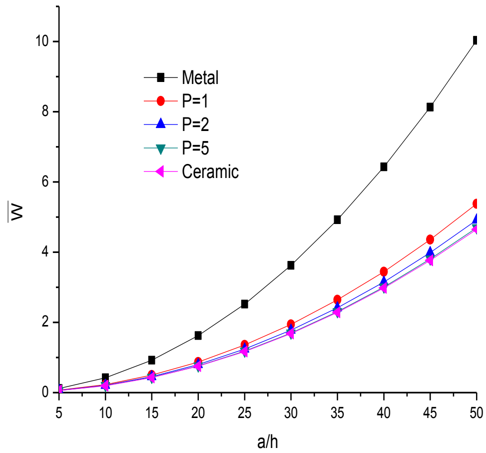

(d) The 1-0-1 FGM sandwich plate

Fig. 6 Dimensionless center deflection $\overline{w}$ as a function of side-to-thickness ratio a/h of FGM sandwich plate (Al/ ZrO_2) with homogeneous softcore for various values of *P* and different types of sandwich plates
- Present model 1 -

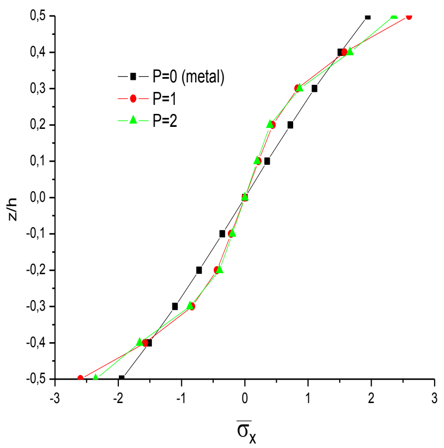

(a) The 1-2-1 FGM sandwich plate

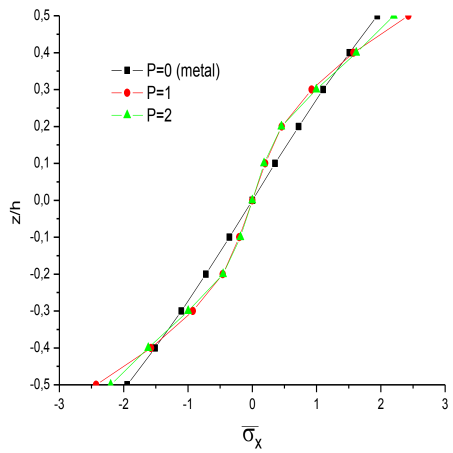

(b) The 1-1-1 FGM sandwich plate

Fig. 7 Variation of normal stress $\overline{\sigma}_x$ through plate thickness of FGM sandwich plate (Al/ ZrO_2) with homogeneous softcore for various values of *P* and different types of sandwich plates (*a/h*=10)
- Present model 1 -

with a homogeneous soft core, transverse deflection decreases as power law exponent *P* is increased. The homogeneous plate (*P*=0) yields the maximum compressive (tensile) stress at the bottom (top) surface. The

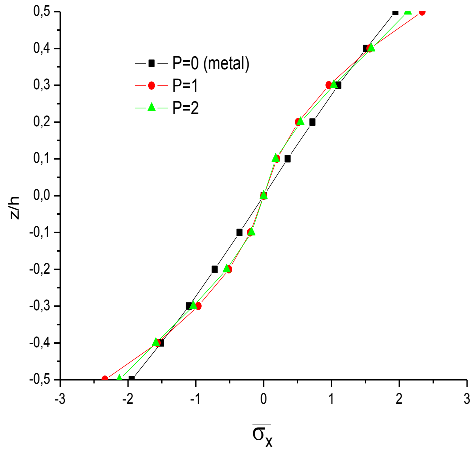

(c) The 2-1-2 FGM sandwich plate

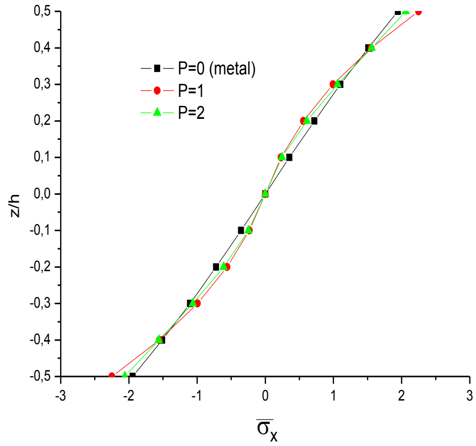

(d) The 1-0-1 FGM sandwich plate

Fig. 7 Continued

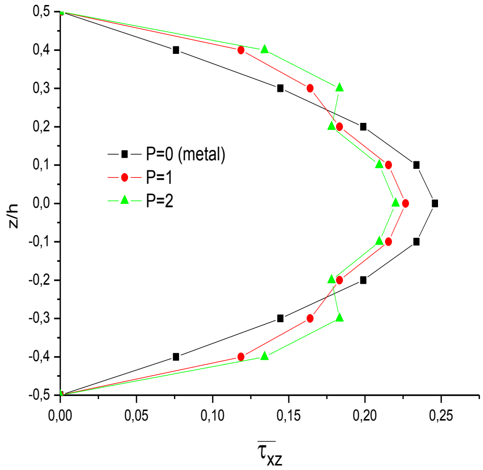

(a) The 1-2-1 FGM sandwich plate

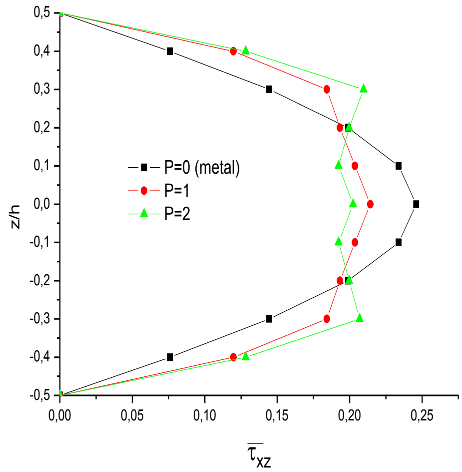

(b) The 1-1-1 FGM sandwich plate

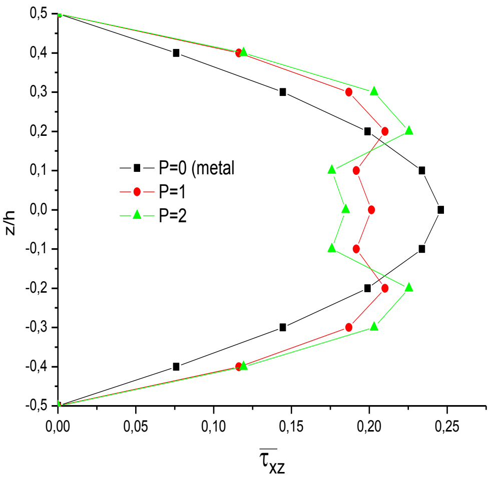

(c) The 2-1-2 FGM sandwich plate

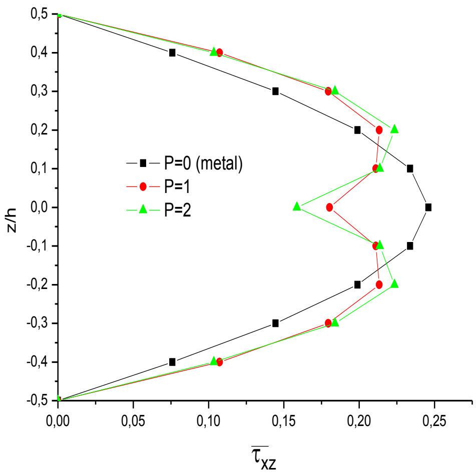

(d) The 1-0-1 FGM sandwich plate

Fig. 8 Variation of transverse shear stress $\overline{\tau}_{xz}$ through plate thickness of FGM sandwich (Al/ ZrO_2) plate with homogeneous softcore for various values of *P* and different types of sandwich plates (*a/h*=10)
- Present model 1 -

homogeneous plate (*P*=0) yields the minimum compressive (tensile) stress at the bottom (top) surface. The stress profile for plate made of pure material (*P*=0) changes linearly through the thickness (Fig. 7). However, the axial stress

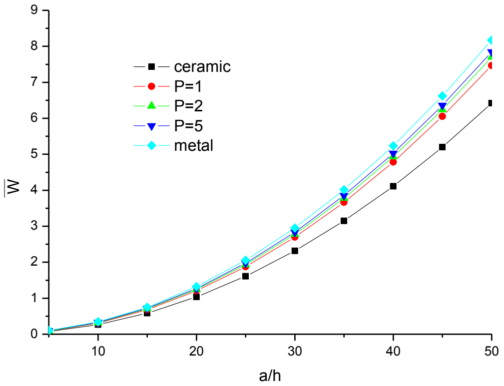

Fig. 9 Dimensionless center deflection $\overline{w}$ of the 1-4-1 sandwich square plate with FGM core. (Al/ ZrO_2)
- Present model 1 -

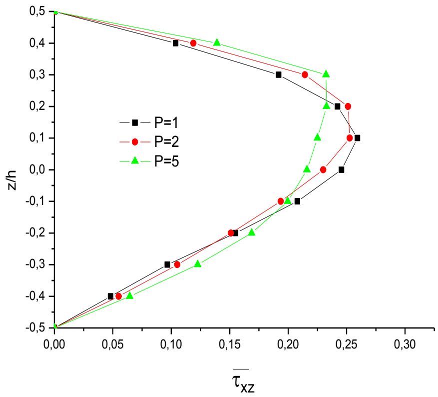

Fig. 11 Dimensionless transverse shear stresses $\bar{\tau}_{xz}$ of the 1-4-1 sandwich square plate with FGM core (Al/ ZrO_2) (*a*/*h*=10) - Present model 1 -

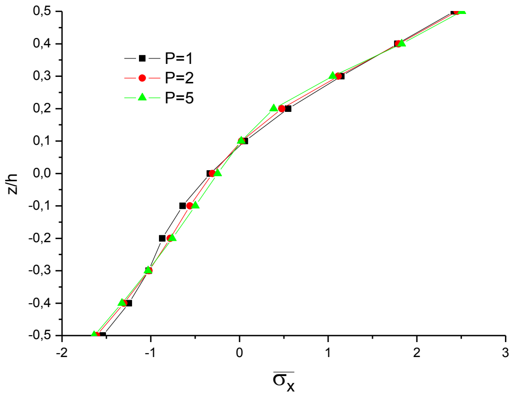

Fig. 10 Dimensionless axial stresses $\bar{\sigma}_x$ of the 1-4-1 sandwich square plate with FGM core (Al/ ZrO_2) (*a*/*h*=10) - Present model 1 -

variation is not linear for FGM plate. Fig. 8 show the plot of shear stress across the FGM (Al/ ZrO_2) plate, the maximum value occurs at a point on the mid-plane of the plate and its magnitude for homogeneous metal plate (*P*=0) is larger than that for FGM (Al/ ZrO_2) plate. Using the first present model (Hyperbolic Shear Deformation Theory) we present in Figs. 9-11 for the (1-4-1) sandwich square plate with FGM core (Al/ ZrO_2) (FGM core) with *P*=1, 2, 5, In this case, the FGM core is metal-rich at the top face and ceramic-rich at the bottom face. The FGM plate deflection is between those of plate made of ceramic and metal (Fig. 9), than the axial stress is compressive throughout the plate up and then they become tensile. The maximum compressive stresses occur at a point on the bottom surface and the maximum tensile stresses occur, of course, at a point on the top surface of the FGM plate (Fig. 10). And the distribution of the shear stress is not symmetric in the case of sandwich plate (Fig. 11).

4. Conclusions

In this paper a new models quasi-3D (Model 1: Hyperbolic and Model 2: Parabolic) shear deformation theory accounting for through-the-thickness deformations was presented. Bending deformations of functionally graded sandwich plates were analysed. The theory accounts for the stretching and shear deformation effects without requiring a shear correction factor. By dividing the transverse displacement into bending, shear and stretching components, the number of unknowns and governing equations of the present theory is reduced to five and is therefore less than alternate theories available in the scientific literature. The governing equations and boundary conditions are derived by employing the principle of virtual work. These equations are solved via a Navier-type, closed form solution, for FG plates subjected to transverse bi-sinusoidal load for simply supported boundary conditions. It is evident from the present analyses; the thickness stretching effect is more pronounced for thick plates and it needs to be taken into consideration in more physically realistic simulations. The numerical results are compared with 3D exact solution and with other higher-order shear deformation theories, and the superiority of these presents theories can be noticed. in the light of the results, we can say that the proposed theories are not only accurate but also efficient in predicting the deflection and stresses of FGM sandwich plates into account the effect of stretching thick.

Acknowledgments

The authors thank the referees for their valuable comments.

References

Abdelhak Z., Hadji, L., Hassaine Daouadji, T. and Adda bedia, E.A. (2015), “Thermal buckling of functionally graded plates using a n-order four variable refined theory”, *Adv. Mater. Res.*, **4**(1), 31-44.

Ait Amar, M., Abdelaziz, H. and Tounsi, A. (2015), “An efficient and simple refined theory for buckling and free vibration of exponentially graded sandwich plates under various boundary conditions”, *J. Sandw. Struct. Mater.*, **16**, 293-318.

Bellifa, H., Benrahou, K., Houari, S.A. and Tounsi, A. (2015), "Bending and free vibration analysis of functionally graded plates using a simple shear deformation theory and the concept the neutral surface position", *J. Braz. Soc. Mech. Sci. Eng.*, **38**(1), 265-275.

Benferhat, R., Hassaine Daouadji, T. and Said Mansour, M. (2015), "A higher order shear deformation model for bending analysis of functionally graded plates", *Tran. Indian Inst. Metal.*, **68**(1), 7-16

Bennoun M., Houari S.A. and Tounsi, A. (2016), "A novel five variable refined plate theory for vibration analysis of functionally graded sandwich plates", *Mech. Adv. Mater. Struct.*, **23**(4), 423-431.

Benyoucef, S., Mechab, I., Tounsi, A., Fekrar, A., Ait Atmane, H. and Adda Bedia, E.A. (2010), "Bending of thick functionally graded plates resting on Winkler-Pasternak elastic foundations", *Mech. Comp. Mater*., **46**, 425-34.

Bouazza, M., Amara, K., Zidour, M. and Tounsi, A. (2014), "Hygrothermal effects on the postbuckling response of composite beams", *Am. J. Mater. Res.*, **1**(2), 35-43.

Bouazza, M., Amara, K., Zidour, M. and Tounsi, A. (2015), "Postbuckling analysis of functionally graded beams using hyperbolic shear deformation theory", *Rev. Inform. Eng. Appl.*, **2**(1), 1-14.

Bouazza, M., Amara, K., Zidour, M. and Tounsi, A. (2015), "Postbuckling analysis of nanobeams using trigonometric Shear deformation theory", *Appl. Sci. Report.*, **10**(2), 112-121.

Bouderba, B., Houari, S.A. and Tounsi, A. (2013), "Thermomechanical bending response of FGM thick plates resting on Winkler-Pasternak elastic foundations", *Steel Compos. Struct.*, **14**(1), 85-104.

Bourada, M., Kaci, A., Houari, S.A. and Tounsi, A. (2015), "A new simple shear and normal deformations theory for functionally graded beams", *Steel Compos. Struct.*, **18**(2), 409-423.

Carrera, E., Brischetto, S., Cinefra, M. and Soave, M. (2011), "Effects of thickness stretching in functionally graded plates and shells", *Compos. Part B: Eng*., **42**, 23-133.

Delale, F. and Erdogan, F. (1983), "The crack problem for a nonhomogeneous plane", *J. Appl. Mech.*, **50**, 609-614.

Della Croce, L. and Venini, P. (2004), "Finite elements for functionally graded Reissner-Mindlin plates", *Comput. Meth. Appl. Mech. Eng*., **193**, 705-25.

Hamidi, A., Houari, S.A., Mahmoud, S.R. and Tounsi, A. (2015), "A sinusoidal plate theory with 5-unknowns and stretching effect for thermomechanical bending of functionally graded sandwich plates", *Steel Compos. Struct.*, **18**(1), 235-253.

Hassaine Daouadji, T., Tounsi, A. and Adda Bedia, E.A. (2013), "Analytical solution for bending analysis of functionally graded plates", *Scientia Iranica, Tran. B: Mech. Eng*., **20**, 516-523.

Lo, K.H., Christensen, R.M. and Wu, E.M. (1977), "A high-order theory of plate deformation-part 2: laminated plates", *ASME J. Appl. Mech*., **44**, 669-74.

Mahi, A., Adda Bedia, E.A. and Tounsi, A. (2015), "A new hyperbolic shear deformation theory for bending and free vibration analysis of isotropic, functionally graded, sandwich and laminated composite plates", *Appl. Math. Model.*, **39**, 2489-2508.

Mantari, J.L. and Guedes Soares, C. (2014), "A trigonometric plate theory with 5-unknowns and stretching effect for advanced composite plates", *Compos. Struct.*, **107**, 396-405.

Marur, P..R. (1999), "Fracture behaviour of functionally graded materials", PhD Thesis, Auburn University, Alabama.

Mindlin, R.D. (1951), "Influence of rotary inertia and shear on flexural motions of isotropic elastic plates", *ASME J. Appl. Mech*., **18**, 31-8.

Nelson, R.B. and Lorch, D.R. (1974), "A refined theory for laminated orthotropic plates", *ASME J. Appl. Mech*., **41**, 177-84.

Neves, A.M.A., Ferreira, A.J.M., Carrera, E., Roque, C.M.C., Cinefra, M. and Jorge, R.M.N. (2012), "A quasi-3D sinusoidal shear deformation theory for the static and free vibration analysis of functionally graded plates", *Compos. Part B: Eng*., **43**, 711-25.

Qian, L.F., Batra, R.C. and Chen, L.M. (2004), "Static and dynamic deformations of thick functionally graded elastic plates by using higher-order shear and normal deformable plate theory and meshless local Petrov-Galerkin method", *Compos. Part B: Eng*., **35**, 685-97.

Rashidi, M.M., Shooshtari, A. and Anwar Bég, O. (2012), "Homotopy perturbation study of nonlinear vibration of Von Kármán rectangular plates", *Comput. Struct*., **106-107**, 46-55.

Reddy, J.N. (1984), "A simple higher-order theory for laminated composite plates", *ASME J. Appl. Mech*., **51**, 745-52.

Reddy, J.N. (2000), "Analysis of functionally graded plates", *Int. J. Numer. Meth. Eng.*, **47**, 663-84.

Reissner, E. (1945), "Reflection on the theory of elastic plates", *ASME J. Appl. Mech*., **38**, 1453-64.

Thai, H.T. and Kim, S.E. (2013), "A simple quasi-3D sinusoidal shear deformation theory for functionally graded plates", *Compos. Struct*., **99**, 172-80.

Tlidji, Y., Hassaine Daouadji, T., Hadji, L., Tounsi, A. and Adda Bedia, E.A. (2014), "Elasticity solution for bending response of functionally graded sandwich plates under thermo mechanical loading", *J. Therm. Stress*, **37**, 852-869.

Tounsi, A., Houari, S.A., Benyoucef, S. and Adda Bedia, E.A. (2013), "A refined trigonometric shear deformation theory for thermoelastic bending of functionally graded sandwich plates", *Aerospace Sci. Technol.*, **24**, 209-220.

Tounsi, A., Menaa, R., Mouaici, F., Mechab, I., Zidi, M. and Adda Bedia, E.A. (2012), "Analytical solutions for static shear correction factor of functionally graded rectangular beams", *Mech. Adv. Mater. Struct*., **19**, 641-52

Zenkour, A. (2007), "Benchmark trigonometric and 3-D elasticity solutions for an exponentially graded thick rectangular plate", *Arch. Appl. Mech*., 77, 197-214.

CC